Mycol. Res. **108** (11): 1241–1256 (November 2004).
DOI: 10.1017/S0953756204001261 *Printed in the United Kingdom.*

Simulating colonial growth of fungi with the Neighbour-Sensing model of hyphal growth

Audrius MEŠKAUSKAS[1], Mark D. FRICKER[2] and David MOORE*[1]

[1] *School of Biological Sciences, Stopford Building, University of Manchester, Oxford Road, Manchester M13 9PT, UK.*
[2] *Department of Plant Sciences, University of Oxford, South Parks Road, Oxford OX1 3RB, UK.*
E-mail: *david.moore@man.ac.uk*

Received 16 May 2004; accepted 8 August 2004.

The Neighbour-Sensing model brings together the basic essentials of hyphal growth kinetics into a vector-based mathematical model in which the growth vector of each virtual hyphal tip is calculated by reference to the surrounding virtual mycelium. The model predicts the growth pattern of many hyphae into three spatial dimensions and has been used to simulate complex fungal fruit body shapes. In this paper we show how the Neighbour-Sensing model can simulate growth in semi-solid substrata like agar or soil, enabling realistic simulation of mycelial colonies of filamentous fungi grown in 'Petri-dish style' experimental conditions. Newly implemented capabilities in the model include: a measurement and logging system within the program that maintains basic statistics about the mycelium it is simulating, this facilitates kinetic experimentation; inclusion of 'substrates' in the data space causing positive or negative tropisms for the growing mycelium; a horizontal plane tropism that provides a way of simulating colonies growing in or on a substratum like agar or soil by imposing a horizontal constraint on the data space the cyberhyphal tips can explore; three categories of hypha – standard hyphae are those that start the simulation, leading hyphae can emerge from the colony peripheral growth zone to take on a leading role, and secondary hyphae are branches that can arise late, far behind the peripheral growth zone, when mature hyphal segments resume branching to in-fill the older parts of the colony. We show how the model can be used to investigate hyphal growth kinetics *in silico* in experimental scenarios that would be difficult or impracticable *in vivo*. We also show that the Neighbour-Sensing model can generate sufficiently realistic cord-like structures to encourage the belief that this model is now sufficiently advanced for parameters to be defined that simulate specific *in silico* cyberfungi. The potential utility of these cyberspecies is that they provide a means to model the morphogenetic effects of a variety of factors, from environmental and nutritional features to mutations, in experimentally realistic situations, offering a valuable addition to the experimental toolkit of all those interested in fungal growth and morphology.

INTRODUCTION

We have recently described a mathematical model of hyphal growth, called the Neighbour-Sensing model, and a Java™ computer program realisation of it that together generate realistic visualizations of filamentous hyphal growth (Meškauskas, McNulty & Moore 2004). The Neighbour-Sensing model brings together the basic essentials of hyphal growth kinetics into a vector-based mathematical model in which the growth vector of each virtual hyphal tip is calculated at each iteration of the algorithm by reference to the surrounding virtual mycelium. Effectively, the mathematics allows the virtual hyphal tip to sense the neighbouring mycelium, which is why we call it the Neighbour-Sensing model. Kinetic hyphal growth equations relate hyphal length, number of branches and growth rate, and incorporation of the influence of external factors on the direction of hyphal growth and branching (i.e. tropisms) provides us with a cyberfungus that can be used for experimentation on the theoretical rules governing hyphal patterning. The Neighbour-Sensing model employs a variety of tropisms (Meškauskas *et al.* 2004) by incorporating mathematical representations of the nature of the signal, its propagation through the medium, and its attenuation; the mathematical model deals with these as abstractions.

There are a range of mathematical models of fungal growth in the literature, and it is worth making a brief comparison between the Neighbour-Sensing model and other fungal models explicitly designed to simulate colony morphology. There are several 'continuous

* Corresponding author.

models' that seek to model the collective attributes of the mycelium, rather than the growth of individual hyphae, but include morphological features such as tip growth, branching, anastomosis and cell death (Edelstein 1982, Edelstein & Segal 1983, Edelstein-Keshet & Ermentrout 1989, Davidson *et al.* 1996, Davidson 1998, Davidson & Olsson 2000, Boswell *et al.* 2002, 2003b). In such models growth is driven by nutrient concentration derived from uptake and internal passive or active transport. These models provide good descriptions of mass and substrate distributions for growth in both homogeneous and heterogeneous environments, but can only describe the topology architecture of the mycelium through its average properties and do not have an explicit morphological representation.

Regalado *et al.* (1996) combined a model of nutrient depletion with a two-dimensional (2D) reaction-diffusion ('Meinhardt') model based on a (hypothetical) autocatalytic activator produced in response to high nutrient levels that promotes tip growth balanced by a (hypothetical) inhibitor that counteracts the activator. This generates 2D representations on a grid of the mycelial structure and generated fractal-like structures. The system responded to experimental variation in nutrient supply.

Ermentrout & Edelstein-Keshet (1993) developed a basic stochastic cellular automaton model of mycelial growth, branching and death, whilst Liddell & Hansen (1993) extended this type of model to include nutrient uptake.

Several attempts have been made to produce morphologically realistic models. Hutchinson *et al.* (1980) modelled *Mucor hiemalis* growing on solid media. The simulation was based on a sampling of measured growth rates, internodal distances and branching angles. Yang, Reichl & Gilles (1992b) simulated 3D pellet formation in *Streptomyces tendae*. The specific growth rate, tip extension rate, frequency distribution of tip angles (normal distribution mean 0.2 ± 10.1) and branch angles (mean 1.2 ± 29.1, measured normal to the growth direction) were measured experimentally. Simulation used random angles drawn from these distributions. Yang *et al.* (1992a) extended this model to include regulation of hyphal tip extension by internal diffusion of a growth limiting nutrient, constrained by septation. Simulations ran for 13 h.

Lejeune and co-workers (Lejeune, Nielsen & Baron 1995, Lejeune & Baron 1997) developed a growth model for *Trichoderma reesei* based on saturation kinetics for hyphal growth and random branching drawn from a measured frequency distribution. The 3D morphology assumed that growth orientation varied stochastically to give curved hyphal growth, the branching location was determined stochastically along the length of the hypha with branch extension was in a plane at 90° from the parent hypha at a random angle in this plane. The tip extension rate was dependent on the level of O_2, with a consumption term included for growth. The fractal dimension of the simulation was measured. Simulations ran for up to 27 h.

López & Jensen (2002) modelled *Aspergillus oryzae* grown on solid media using a 2D lattice with probabilities of growth being related to the age of the nearest neighbour and supply of nutrients, and inhibition by accumulation of toxic waste products spreading by diffusion. No explicit branch structures are formed in the model but it simulates changes in the colony margin.

By far the most visually realistic simulations of plant development have been produced using 'Lindenmayer'- (or L-) systems. L-systems are string rewriting rules (productions) operating on a component (predecessor) and converting it to a successor according to the rule(s), so that a complex object can be developed by successive replacement of parts of a simpler object. They were formulated by Aristid Lindenmayer (Lindenmayer 1968) as an axiomatic theory of biological development. L-systems operate with a string notation which has been given increasing levels of complexity and simulation power over the years (Prusinkiewicz & Lindenmayer 1990, Prusinkiewicz 1994, 2004; *Visual Models of Morphogenesis* website at http://algorithmicbotany.org/vmm-deluxe/).

Although branching fungal mycelia fit well with the L-system framework there has been remarkably little application of L-systems to modelling fungi. Liddell & Hansen (1993) produced a simple L-system with stochastic variation in branching angle that created a 2D pattern with some similarity to early mycelial growth. They then went on to develop a cellular automata model of branching patterns to incorporate interactions with anisotropic nutrient availability. Soddell, Seviour & Soddell (1995) developed a stochastic parametric L-system to model different *Mucor* species, with variation in branching angles, hyphal orientation, interbranch distances and growth rates, but no endogenous control or sensitivity to environmental factors. The parameters were based on experimental data and the resultant simulations generated realistic images by visual inspection. Tunbridge & Jones (1995) produced an elegant stochastic parametric L-system to simulate growth of *Aspergillus nidulans* built on a mechanistic explanation of the underlying cellular processes originally put forward by Prosser & Trinci (1979). In this context-sensitive parametric L-system, tip growth is dependent on vesicle supply from subapical segments. Once sufficient growth occurs, nuclear division and septum formation take place. If sufficient vesicles subsequently accumulate in subapical segments, branch formation is initiated. Iteration of these rules generates a string describing the branching structure, but with no explicit 2D or 3D representation. To produce realistic 2D images, additional stochastic operations were included during visualization of the structure, such as random selection of branching direction, variation in branching angle, curved hyphal shape and preferential radial growth. The authors note that more realistic

graphical depiction would require introduction of geometrical information into the simulation so that the stochastic elements form part of the developmental rules rather than just affecting visualization of the structure.

These extended L-systems and the Neighbour-Sensing model are trying to solve similar problems with fairly similar approaches. The main differences reside in the notation used to describe the representation of components in the models. Also, in the classic L-systems no mechanisms exist to rearrange a set of existing cells (these models deal primarily with plant and algal morphogenesis, where cells are tightly bound together). Fungal cells, especially hyphal tips, do change position during development of a structure and L-systems are comparatively less suited to simulating fungal morphogenesis. Even extended L-systems have difficulty coping with formation of a structure by rearranging existing cells, as occurs, for example, in aggregation of existing hyphae to develop fungal cords and fruit bodies. The Neighbour-Sensing model describes each active agent (hyphal tip) by its 3D position, length, and growth vector rather than a string. At each iteration of the algorithm the tip advances according to a set of rules and its interaction with the local fields, some of which are directed (vector) fields. In both cases the user has to establish a set of basic rules on growth rates, branching angles and interactions with fields, but the Neighbour-Sensing model deals with active agents (which are given biological characteristics) that are independent of the programmer, whereas L-systems deal with geometrical forms which the experimenter-programmer defines and then adjusts to refine the simulation. In the Neighbour-Sensing program each hyphal tip is an active agent that is allowed to vector within 3D data space using rules of exploration that are set (initially by the experimenter) within the program. Those Neighbour-Sensing rules are the biological characteristics. They start with the basic kinetics of in vivo hyphal growth, include branching characteristics (frequency, angle, position), and, through the tropic field settings, involve interaction with the environment. A graphical user interface (GUI) written into the Java™ realisation of the Neighbour-Sensing model makes adjustment of the parameters an easy operation for even the casual user of the program, but the geometrical form of the outcome of a Neighbour-Sensing program run is not defined by the experimenter – it is not a painting program. Rather, the final geometry must be reached by adapting the biological characteristics of the active agents during the course of their growth. Exactly as in life.

The key features that distinguish the Neighbour-Sensing model are:

(1) The mycelial morphology is explicit and three-dimensional.

(2) The branching frequency, position and orientation are now determined directly by model components, rather than through a random stochastic process, (although the user can add additional probability factors on branching if required).

(3) Regulation of growth and branching occurs in response to evaluation of local density-dependent fields. The most important field (negative autotropism) is an abstract representation of growth inhibition from substrate depletion or accumulation of toxic waste-products. The secondary long-range autotropism has no well-documented physical representation, but represents the type of interaction that might arise from diffusible signalling molecules.

(4) The impact of external fields, such as gravity, and physical constraints are included.

These features form the 'parameters' of the model, and all are under the control of the user via the GUI.

It is often useful in these discussions to refer to a specific tropism by name, but the visualizations result from the abstract mathematical treatment of physical parameters. Consequently, reference to a specific tropism in the text should be understood to stand for a signal of similar physical parameters rather than be a prediction for the involvement of that specific signal.

As described so far, the Neighbour-Sensing model predicts the growth pattern of many hyphae into three spatial dimensions and this capability was used in a series of model experiments to show that complex fungal fruit body shapes can be simulated by applying the same regulatory functions to all of the growth points active in a structure at any specific time – the shape of the fruit body emerging from the concerted response of the entire population of hyphal tips, in the same way, to the same signals.

However, most mycologists are more familiar with fungal mycelia grown under some form of growth restraint, the most usual being colonies grown on the surface of agar media in containers of restricted size. In this report we show how the Neighbour-Sensing model can simulate growth in semi-solid substrata like agar or soil, and we also take the opportunity to introduce a number of other parameters and modelling capabilities that permit initial experimentation on hyphal growth kinetics, and enable realistic simulation of mycelial colonies of filamentous fungi grown in 'Petri-dish style' experimental conditions. We also discuss the opportunities that might exist for incorporation of hyphal anastomoses in the model, and the inclusion of physiological processes such as nutrient uptake and translocation.

MATERIALS AND METHODS

Refer to Meškauskas *et al*. (2004) for basic information about the mathematics underlying the Neighbour-Sensing model. Here we will describe only the further developments relevant to the present study.

Mycelial statistics

We have implemented a measurement and logging system within the program by which the program maintains basic statistics about the mycelium it is simulating. With the current version of the program we can measure total mycelial length (which is proportional to total mycelial mass), internode length, internode age, tip age and the values of the various fields generated by the parameter set used during the course of a simulation. The model can also return values for the distance between the two most remote points of the mycelium, so the extension growth rate of the mycelium can be measured (as opposed to the hyphal tip extension rate, which is set in the program to unity). Output of such statistics permits *in silico* experiments analogous to those performed *in vitro*. However, by tracking changes in parameters across a wide range of possible scenarios, the model makes it considerably easier to extrapolate from conditions where it may be easy, although time-consuming, to make measurements of morphological features, to situations that are much more difficult to analyse *in vivo*. We show below, as an example, how the hyphal growth unit and peripheral growth zone of a colony are affected as the spherical morphology is constrained to a flattened circular disk – simulating the difference between submerged liquid culture and Petri dish culture.

Substrates

The data space of the published model is a three dimensional environment occupied only by the cybermycelium 'growing' in accordance with the parameter rules set by the user of the program. We have now added to this the opportunity to include numerous additional objects ('substrates') to the model space, each of which generates its own field, causing positive or negative tropism for the growing mycelium. The substrate, T, contains the centre co-ordinates, T_{center}, the radius (T_R) and the impact factor (T_{impact}). T_{impact} can be positive or negative (the latter for inhibitory substrates). If needed, all parameters can be interactively altered during the simulation. The field of the substrate T is equal to:

$$O_{T,p} = T_{impact}\Psi(|p - T_{center}| - T_R)\frac{1}{|T_{center} - p|^2} \quad (1)$$

where Ψ is a Heaviside function. In other words, the field of the substrate is similar to the first type of hyphal field, but T_{impact}-times stronger than the field of the single hyphal segment (length l_c). It is equal to zero if the point of interest is inside the substrate.

The field of all substrates at the point of interest p is:

$$O_p = \sum_{\forall T} T_p \quad (2)$$

Symbols and terminology used in equations (**1**) and (**2**) are described in Meškauskas *et al*. (2004).

Here again we do not want our choice of terminology to limit the evident scope of the program. We describe a volume of the data space, presently defined as a sphere, able to attract hyphal tips as a 'substrate', a volume able to repel hyphae as an 'inhibitor'. There is no limit on the number of substrates used in a simulation (other than the effect of computational load on computer performance), nor is there a limit on the relative abundance of substrates *versus* inhibitors. Substrates can be positioned anywhere within the data space, and can be added to or subtracted from an ongoing simulation by pausing the simulation and altering the parameters. By appropriate choice of characteristics it is possible to assign to the substrates the features of non-nutrients. For example, an inhibitory substrate that is set to be totally inhibitory is equivalent to a physical barrier, while a substrate can also be interpreted as analogous to locally-diffusing morphogens, the field they generate (and to which the hyphal tips react) being equivalent to the diffusion gradient of a morphogen.

Horizontal plane tropism

Tropisms are implemented in the Neighbour-Sensing model using the concept of a field to which growing hyphal tips react, the different tropisms being distinguished by the different physical characteristics ascribed to the field. For example, for the hyphal density field, which can be used to implement an autotropism, it is supposed in the model that each point of the mycelium contributes to a field that can be described by the formulas used to describe electric and gravitational fields in physics. The program implements positive and negative autotropic reactions by orienting the growing hyphal tip towards or against the gradient of this field, and the user also controls whether tip growth, branching, or both are reactive. The published model features six tropisms: negative autotropism, based on the hyphal density field; secondary long range autotropism (that attenuates with either direct or inverse proportionality to the square root of distance); tertiary long range autotropism, which attenuates as rapidly as the negative autotropism but can be given a large impact value; two galvanotropisms based on the physics of an electric field produced by the hypha which is parallel to the hyphal long axis; and a gravitropism, which orients hyphae relative to the vertical axis of the user's monitor screen.

Fundamentally, the Neighbour-Sensing model adopts a phenomenological approach to capture observable macro-level effects for which the underlying mechanistic cause may not be known, and may depend on complex interactions of several factors. For example, negative autotropism has been suggested to arise from depletion of nutrients or oxygen levels, build-up of toxins, propagation of inhibitory signalling molecules, interaction of electric fields, or a combination of all of these. Rather than formulate equations to describe

each of these potential influences, we infer that the magnitude of the autoinhibitory domain will depend on the number of adjacent tips or the local density of mycelium. Thus the Neighbour-Sensing model encapsulates the concept of a local density-dependent inhibitory field with an inverse-square dependence on distance without specifying the precise causal agents (so the model can predict the potential influence of such agents leaving the experimenter to identify them *in vivo*). This approach captures the instantaneous influence of neighbouring tips and/or mycelium, but does not currently deal with any time-dependent changes in the development of the autoinhibitory fields that could be anticipated during nutrient depletion or accumulation of toxins, for example. This approximation is likely to be valid near the colony margin where most growth and branching takes place, as the growth process continuously invades new territory before the activity of the mycelium has significantly perturbed the local environment. Growth and branching therefore take place under quasi steady-state conditions along a gradient from the bulk medium to the interior of the colony. The level of interaction can be represented as a single parameter scaled by the local density of the mycelium (or number of tips). Section age is included in the description of each section of hypha and can be used to impose additional constraints on branching once a threshold value is exceeded. It would be possible to incorporate this as a continuous weighting function to model time-dependent increase in the autoinhibitory field.

Of the tropisms explicitly named, gravitropism should be uncontentious as there is considerable evidence for response by fungi to this physical field, even though the mechanism of gravity perception and reaction in fungi is not known (Moore 1991, Moore *et al*. 1996). Likewise, we provide below reference to the likely origin and influence of electric fields leading to the inclusion of a galvanotropic field. Other fungal tropisms (including potential 'growth hormones' and/or 'morphogens') have been discussed elsewhere (Moore 1984, 1993, 1994, 1998: 246–391, Novak Frazer 1996).

The newly-implemented horizontal plane tropism provides a way of simulating colonies growing in or on a substratum like agar or soil by imposing a horizontal geometrical constraint on the data space the cyberhyphal tips can explore to simulate the physical constraint of the substratum. The user can set the impact (determining how strongly the hyphal tips are limited to the horizontal plane) and the permissible layer thickness (in standard distance units). Mathematically, this feature is implemented in the same way as other tropisms (Meškauskas *et al*. 2004). At the moment, the horizontal tropism constrains the dimension within which the mycelium will expand in a symmetrical fashion. In a future version, we plan to make the constraint asymmetrical to represent colonial growth on the surface of a penetrable substratum.

Hyphal differentiation

The essential element of the Neighbour-Sensing model is a hyphal tip that has four characteristics: position in three-dimensional space; a growth vector; length; and ability to branch. During each iteration of the algorithm the tip advances by a growth vector (initially set by the user) in accordance with the effects of one or more tropic vectors, and may branch (with an initial probability set by the user), also in accordance with the effects of one or more tropisms set by the user. The original model dealt with only one sort of hypha, the current version offers three categories of hypha. In the latest model standard hyphae are those that normally start developing when a simulation is initiated; leading hyphae can emerge from the colony peripheral growth zone (with a probability determined by the user) to take on a leading role (in the formation of cords, as explored below, for example); and secondary hyphae are branches that arise late, far behind the peripheral growth zone, when mature hyphal segments (of either standard or leading hyphae) resume branching to in-fill the older parts of the colony. All hyphal types can be made sensitive to the full range of growth vector regulation, and can be given parameter sets that are different from the other hyphae used in a simulation. The user can also determine the probability that a new branch will become a leading or secondary hypha. Mathematically the different categories of hyphae are implemented as additional objects, and the Java™ program is expanded to provide user interfaces so that parameters can be set individually for each sort of hypha.

Cultivation of Phanerochaete

10 mm^3 beech wood blocks were autoclaved twice and inoculated by placing on colonies of *Phanerochaete velutina*[1] growing on 2% malt agar (2% malt extract; Oxoid, Basingstoke; 2% Oxoid No. 3 agar) at 22 ± 1 °C in darkness in a temperature-controlled incubator (Gallenkamp, Loughborough) for 4 wk. The surface mycelium was lightly scraped from the colonized blocks and they were placed on a 5 mm thick layer of moistened, compressed acid-washed black sand in 24 cm^2 Petri-dishes. Growth was imaged under constant low intensity illumination (Osram 12W) using a Cohu 9120 CCD camera equipped with a Navitor TV zoom lens (Brian Reece Scientific, Newbury). Images were averaged over 50 frames and collected every 2 h for up to 512 h using a Matrox Meteor II framestore controlled by Zeiss KS 300 software (Imaging Associates, Thame).

RESULTS AND DISCUSSION

Program statistics

The program maintains records and collects statistics about the simulation it is creating. Manual adjustments

[1] An original field isolate kindly provided by Lynne Boddy (University of Cardiff) and now deposited in **IMI**.

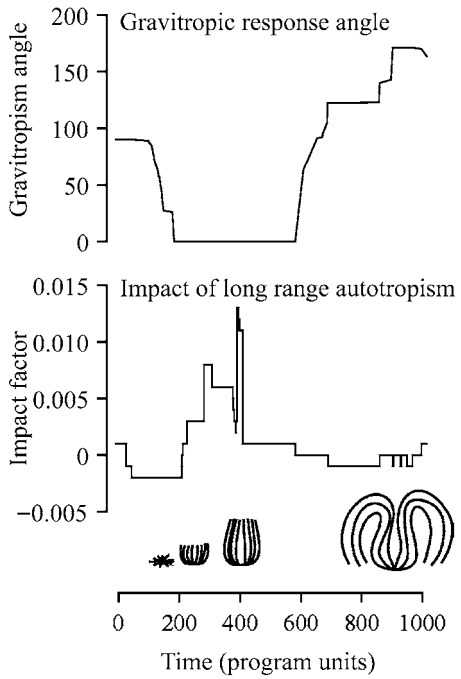

Fig. 1. The Neighbour-Sensing program maintains records and collects statistics about the simulation it is creating. Manual adjustments made to parameters in the program as a structure is created are logged in a text file which develops as a record of the settings for tropic fields and their characteristics over the time during which the visualization develops. This figure shows changes in the major tropisms employed to develop a structure similar to the young fruit body primordium of *Coprinopsis cinereus*. Major parameter settings were: $P_{branch}=40\,\%$, $N_{branch}=0.06$ (density field hypothesis used), field generated by all components of the mycelium, $l_c=20$, k (persistence factor) $=0.1$, I_g (impact of gravitropic component) $=0.0020$ with $\beta_{\text{tolerance}}=\pm 5^{\circ}$. Long range autotropic interaction was inversely proportional to the square root of the distance. The graph records the changes made to the angle of gravitropic reaction and the impact (='strength') of the long range autotropic reaction in order to develop the mushroom primordium from a disk-shaped initial colony. The cartoons at the base of the figure show the morphology of the main stages.

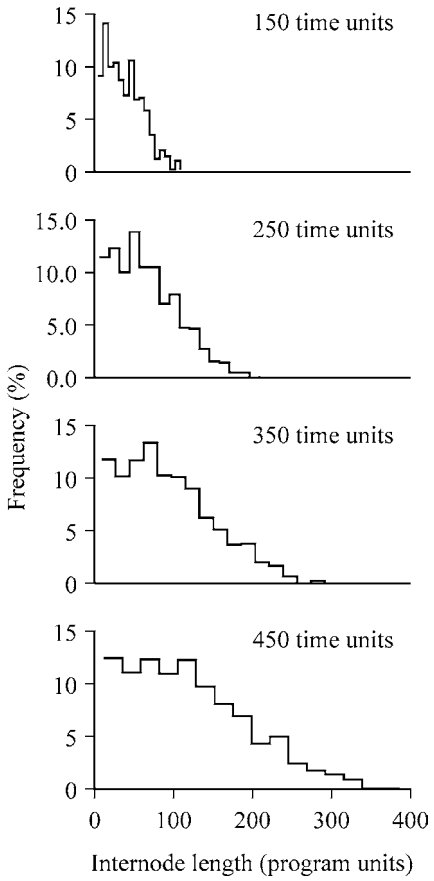

Fig. 2. Statistical distribution of the internode length in the growing spherical colony at various time intervals (numbers above each panel indicate the colony age in relative time units). The growth was simulated assuming negative autotropic reaction (persistence factor $k=0.1$) and density-dependent branching (threshold 0.06), with the density field generated by all of the mycelium ($l_c=20$). If the density allowed branching, the branching probability was 40 % per iteration (=per time unit).

made to parameters in the program as it creates structures in the visualization on the monitor screen are logged in a text file which develops as a record of the settings for tropic fields and their characteristics over the time during which the visualization develops. The text file can then be used by a robot in the program to repeat the set of manipulations exactly, and as explained before (Meškauskas *et al.* 2004), the logic is very similar to the natural logic implied in the expression of a genotype to allow development of a particular phenotype. However, the file can also be retrieved into graph-drawing programs (it is a tab-delimited list) to produce graphs that illustrate how the parameters changed during the development to improve understanding of *how* a 'genotype' produces a 'phenotype'. Fig. 1 shows one such record as a graph that illustrates changes made to the key tropisms (in this case gravitropism and a long range autotropism) to develop a 'mushroom primordium' from a disc-shaped initial colony, which was first shown as Fig. 7 in Meškauskas *et al.* (2004). The structure represented in Fig. 1 was developed on-screen interactively by manual adjustment of parameters. This represents an 'experiment' in use of the Neighbour-Sensing model to develop a particular morphology. Later analysis of the recorded data (Fig. 1) demonstrates that the main features of the structure that emerged developed in four phases: (1) high diagravitropic angle + low impact of the long range autotropism; (2) low angle + increasing impact; (3) low angle + low impact; and (4) increasing angle + low impact. The visualization corresponding to each phase is shown in the cartoons at the base of Fig. 1. Even if the specifically named tropisms are not involved *in vivo*, this sort of analysis focuses attention on exactly how relatively simple alterations in basic tropisms can cause shape and form to arise during fungal morphogenesis. The importance of this exercise is *not* that the experiment claims to show exactly how a

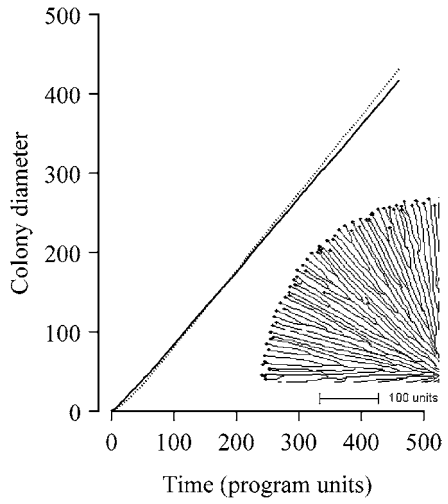

Fig. 3. Effect of growth restriction to a thin layer on the colony extension growth. The dotted line represents growth of the spherical colony, and the solid line growth of the nearly flat colony, where hyphae are forced to stay in a thin layer (four growth units thick) with the horizontal tropism constant set at 0.002. A quadrant of the 'flat' colony is included at bottom right of the figure to illustrate colony morphology; small circles at the ends of branches are flags that identify the position of the apex, in on-screen simulations they are colour-coded red for non-growing and blue for growing tips in the iteration of the algorithm displayed.

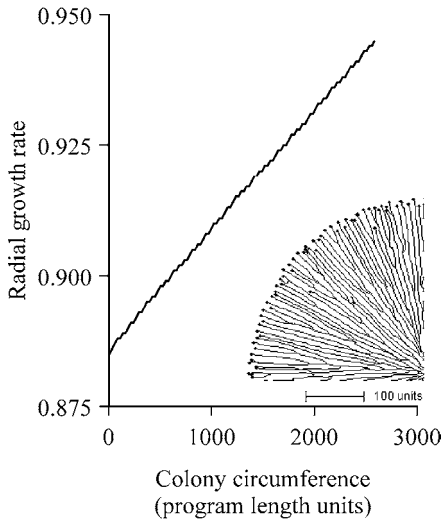

Fig. 4. Radial colony growth rate as a function of the colony circumference. The growth was simulated in a nearly flat colony (as used in Fig. 3), where hyphae were forced to stay in a thin layer (four growth units thick) with the horizontal tropism constant set at 0.002. Other parameters assumed negative autotropic reaction (persistence factor $k=0.1$) and density-dependent branching (threshold 0.06), with the density field generated by all of the mycelium ($l_c=20$). If the density allowed branching, the branching probability was 40% per iteration (=per time unit).

mushroom shape emerges *in vivo*. Indeed, Meškauskas *et al.* (2004) show that there is more than one way to arrive at this shape using the model and this mirrors the diversity of developmental patterns observed among mushrooms in nature (Watling & Moore 1994). Rather, the importance of this experiment is that it shows how *little* control is needed to arrive at a characteristic fungal morphology.

The program also records a range of basic statistics about the mycelium it is simulating. For example, Fig. 2 shows the statistical distribution of the internode lengths in a growing spherical colony at various time intervals. These data make it clear that internode lengths increase with time with the growth and branching regulatory parameters set for this particular visualization. Clearly, easy access to these sorts of measurements allows experiments to be carried out on *in silico* model kinetics for comparison with *in vivo* growth statistics for a range of colony types. Experiment with the model shows that colony radius increases linearly, rather than exponentially, with time (Fig. 3). This is entirely in accord with *in vivo* hyphal growth kinetics. Of course, *in vivo* the growth rate of germ tubes produced by germinating spores accelerates through an exponential phase towards linear kinetics (Prosser 1995). This feature is not incorporated into the current model, but would not be difficult to implement. Similarly, in this simulation the cyberfungus is grown under notionally ideal conditions so the leading hyphal tips do not experience any diminution in growth rate due to exhaustion of resources. However, substrate depletion and/or the accumulation of toxic excretion products behind the colony margin as the mycelial density increases, and which may contribute to a reduction in branching frequency and growth rate, are captured in the density dependent negative autotropism field.

The slope of the line in both cases in Fig. 3 is about 0.86, a little less than the growth rate of the single tip (which is set in the program to $=1.00$). The reason for this is that growing tips are not oriented on strict radii from the colony centre, especially after branching. Model measurements also show that extension growth rate (increase of radius/time interval) is proportional to the circumference of the colony (Fig. 4). These features are not included explicitly in the model's algorithm, but emerge from expression of the algorithm. The fact that they do so emerge demonstrates two important points: first that the model is a realistic *in silico* representation of the *in vivo* fungus; and second, that *in vivo* these features are not themselves directly regulated but are a consequence of the execution of basic fungal growth kinetics.

For the most part the kinetics apply equally to spherical colonies and to those growing under a restriction that limits growth to a flattened colony. The latter morphology is achieved in the model with the horizontal plane tropism. The effect of this tropism on the shape of the colony is illustrated in Fig. 5.

The combination of this tropism with the data-collection ability of the model permits an *in silico* experiment to be carried out which would be impracticable

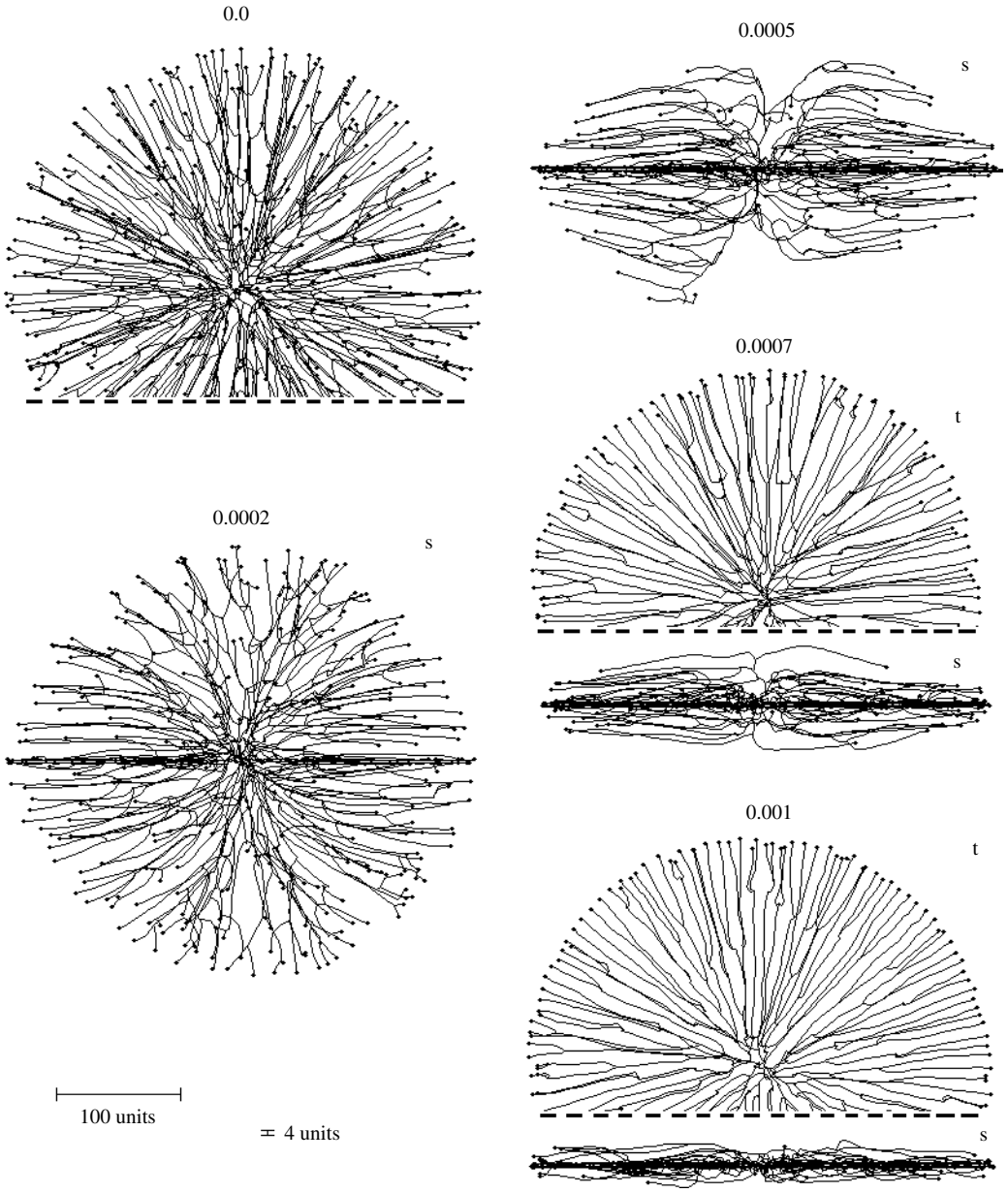

Fig. 5. Effect of the horizontal plane tropism on the shape of the colony. The numbers above the images indicate the selected impact factor (='strength') of the horizontal tropism constant (HTC). With an impact factor of zero the colony is spherical. The thickness of the 'horizontal zone' was set to 4 distance units (see scale bars at bottom left). For some of the symmetrical shapes only part of the view is shown, the dashed line indicating where the image has been cropped. Two viewing angles are shown, s = side view, t = top view. The growth was simulated assuming negative autotropic reaction (persistence factor $k = 0.1$) and density-dependent branching (threshold 0.06), with the density field being generated by all of the mycelium ($l_c = 20$). If the density allowed branching, the branching probability was 40% per iteration (per time unit). The age of all colonies shown is 220 time units.

or impossible *in vivo*: we can determine whether the hyphal growth unit alters as growth pattern changes from spherical to flat-colonial. The model can output total mycelial length and number of branches as the horizontal plane tropism is applied. This experiment shows that forcing mycelia to grow in a thin layer gradually reduces the total length of the hyphae, with the consequence that the hyphal growth unit increases to a peak value (Fig. 6). Mathematically, the horizontal plane tropism is effectively placing a geometrical constraint on the data space available to the cyber-hyphae. In biological terms, Fig. 6 makes it evident that although both branching and extension growth of exploratory hyphae suffer a severe decline as this constraint is applied, the two are uncoupled and branching is more rapidly affected. The consequence of this is a 'spike' representing an increase of 25% in the hyphal growth unit as the colony geometry makes the major transition from more-or-less three dimensional to more-or-less two dimensional.

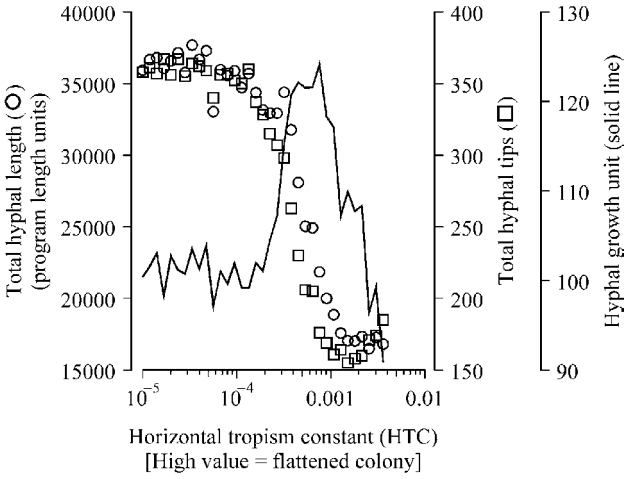

Fig. 6. Effect of the horizontal tropism constant (HTC) on the hyphal growth unit. All growth parameters were the same as in Fig. 5. Forcing mycelia to grow in a thin layer reduces the total length of the hyphae, but has a more drastic effect on the number of hyphal tips. Uncoupling of these features occurs at the transition to '2-dimensional' growth and coincides with the peak of the hyphal growth unit value. Fig. 5 gives a visual guide to the morphology of colonies at various horizontal tropism constants.

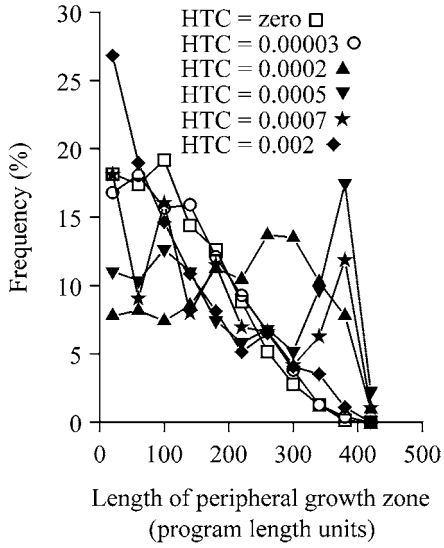

Fig. 7. Effect of colony morphology on the peripheral growth zone. Graphs show distributions of the length of terminal sections that end in a single growing tip (considered to be equivalent to the width of the peripheral growth zone). Data for six colony morphologies are shown, determined by the horizontal tropism constant (HTC), varied from zero (=spherical colony) to 0.002 (which gives a nearly flat, circular colony). The age of all colonies is equal to 460 time units. All other model parameters were the same as in Fig. 5.

The peripheral growth zone is another statistic that is an important character of fungal colonies *in vivo*. It is defined as being equivalent to the length of hypha contributing to tip growth (Prosser 1995). It is generally measured *in vivo* as the length of the spore germ tube at which growth switches from exponential to linear kinetics. As pointed out above, in the present formulation of the Neighbour-Sensing model extension growth rate is uniformly maximal, so there is no meaningful analogue of the *in vivo* experiment. On the other hand, since growth rate *is* set to be maximal in the model, we consider the peripheral growth zone to be equivalent to the length to which the apical segment of the cyberhypha can extend before it meets the requirements for branching (as determined by the parameter set chosen by the user). Consequently, the average length of the segment from the most recent branch to the growing tip *in silico* is analogous to the length of living hypha needed *in vivo* to support the growing tip. The length of this segment is readily logged by the model, so once again, we can undertake experiments that are difficult or impossible with live fungi to demonstrate, for example, that the averaged values for the length of the peripheral growth zone are much the same in spherical (121.7 units) and flat (117.3 units) colonies, but almost doubled in colonies of intermediate shape (204.3 units). Again, the major shift occurs during the final transition to 'flatness' (Fig. 7). As the horizontal tropism constant (HTC) is increased to higher levels it causes an increasing frequency of long terminal segments. At the maximum value of HTC tested the long terminal segment frequency falls back to about that observed in spherical colonies and, instead, there is a significant increase in the frequency of short terminal segments in the flattest colony. The lengths of the terminal segments in each colony type are not normally distributed (Fig. 7). *In silico* this is a consequence of the need for this segment to extend to bring the tip into a locality where it is eligible to branch; *in vivo* non-normal distribution would be a consequence of the need for the terminal segment to be of a length sufficient physiologically to support extension growth of its tip.

Substrate resources

The pattern of growth of all hyphae can be influenced in a localised manner by placing 'substrates' in the growth space. The mycelium in Fig. 8 was grown using negative gravitropism implemented at $-20\,^{\circ}$, but two spheres of an attractive substrate (green) and one of an inhibitory substrate (red at centre) were also added to modify the growth pattern. The slice taken through the vertical centre shows the tips growing around the inhibitory substrate and towards the attractive substrates. Once inside the sphere of influence of the attractive substrates the tips are unable to free themselves until the user removes the substrates from the growth space.

Hyphal differentiation

The program generates its structures by creating and plotting individual hyphal tips. All of the visualizations are made up of hyphal tips, sometimes many thousands, which are expressing independently the growth

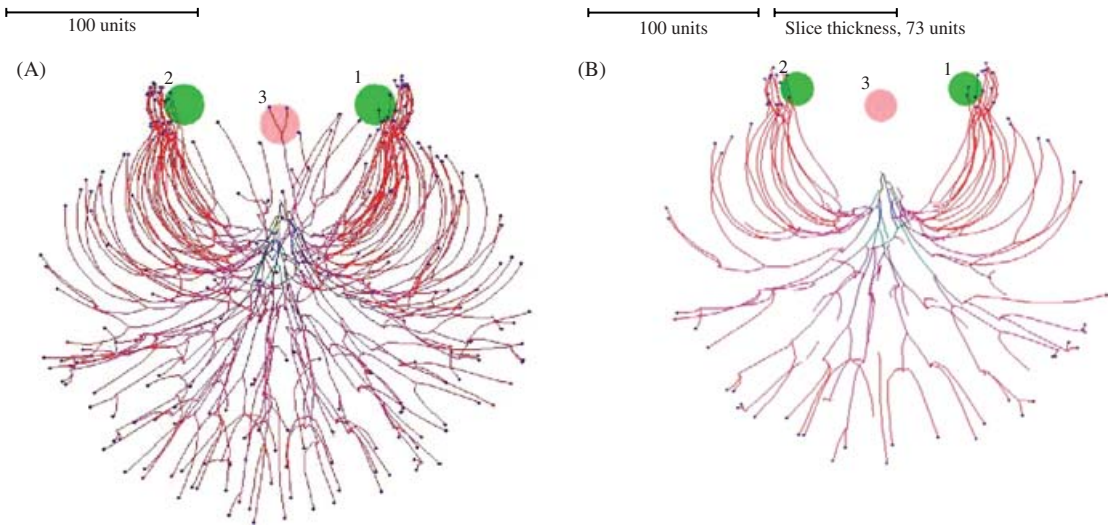

Fig. 8. Inserting substrates and inhibitors into the data space. The parameter set was the same as was used for Fig. 2, but two spheres of attractive (green, and labelled with numerals 1 and 2), and one inhibitory (red, labelled 3) substrates were added to modify the growth pattern further. The field generated by substrates is 1000 times stronger than the field generated by a mycelial segment with a length equal to 20 distance units. The position of the attractive substrates was (50, 0, −50) and (−50, 0, 50), the inhibitory substrate was placed at (0, 0, −40), the radius of all substrates was 20 (all values are given in program distance units). Fig. 8A is a view of the whole (three dimensional) mycelium, and Fig. 8B is a slice through the centre of the object showing how the hyphal tips have avoided the inhibitory substrate and congregated around the attractive ones (tips which appear to be within the inhibitory substrate in Fig. 8A are actually situated above the substrate). Colour of a hyphal segment in these figures depends on the number of growing tips the segment supports, from black (supporting many tips) to red (one tip).

rules that have been assigned to them. Users who wish to inspect the detail of hyphal tip behaviour can zoom into the simulation to do so. The detail can be ignored by zooming out to view overall morphology. The detail can be changed by altering the parameters.

The program offers a number of ways in which hyphae can be differentiated. 'Standard' hyphae are those formed when a simulation is started. 'Leading' hyphae can emerge from the colony peripheral growth zone to take on a leading role in the formation of a linear mycelial structure, for example. 'Secondary' hyphae are branches that arise when mature hyphal segments resume branching in the older parts of the colony. The secondary hypha routine enables the emergence of structures from a colony to be modelled. For example, imposing secondary branching on a planar colony, but releasing the secondary branches from the horizontal plane tropism and making them negatively geotropic instead, results in emergence of randomly distributed fascicles of hyphae growing up from the colony, rather like sporing structures emerging from a Petri dish culture (Fig. 9).

Where hyphal tips are interacting with other hyphae, the trajectory of a hyphal tip that is approaching another hypha under the influence of an autotropism strongly depends on the angle of approach. Alleviation of the negative autotropism causes hyphal aggregation of secondary hyphae but is very sensitive to the branching angle. At acute approach angles, tips curl in a manner that may cause the approaching hyphal tip to curl around its target in a spiral; an obtuse angle results in the approaching tip 'orbiting' its target aimlessly (Fig. 10). Although this results in hyphal aggregation, it is not sufficient to cause formation of more ordered linear structures such as stands, cords and rhizomorphs, so the overall pattern of mycelia generated under these conditions is very different from the known morphology of real mycelia producing cords. On the other hand, this sort of behaviour is rather reminiscent of tendril hyphae and, more generally, of the 'hyphal knots' described by Reijnders (1977, 1993). In the latter, a central inducing hypha is thought to cause a concerted pattern of differentiation in a surrounding family of other hyphae. This is effectively what is happening in the visualization shown in Fig. 10, although the hyphal knot in this case is being expressed in the tropic growth of the surrounding hyphae, rather than by their morphological differentiation. The program, of course, can only simulate *vectorial* differentiation at this time, though it reveals a regulatory strategy by which Reijnders' hyphal knots could be generated.

Mycelial structures

Fungi are able to form several linear structures (strands, cords, rhizomorphs, mushroom stems), which consist of many hyphae growing in parallel in the same direction. Models based only on combinations of negative and positive autotropisms cannot effectively simulate the morphogenesis of such structures because strong positive autotropism (needed to bring the hyphae together) tends to turn the hyphae towards

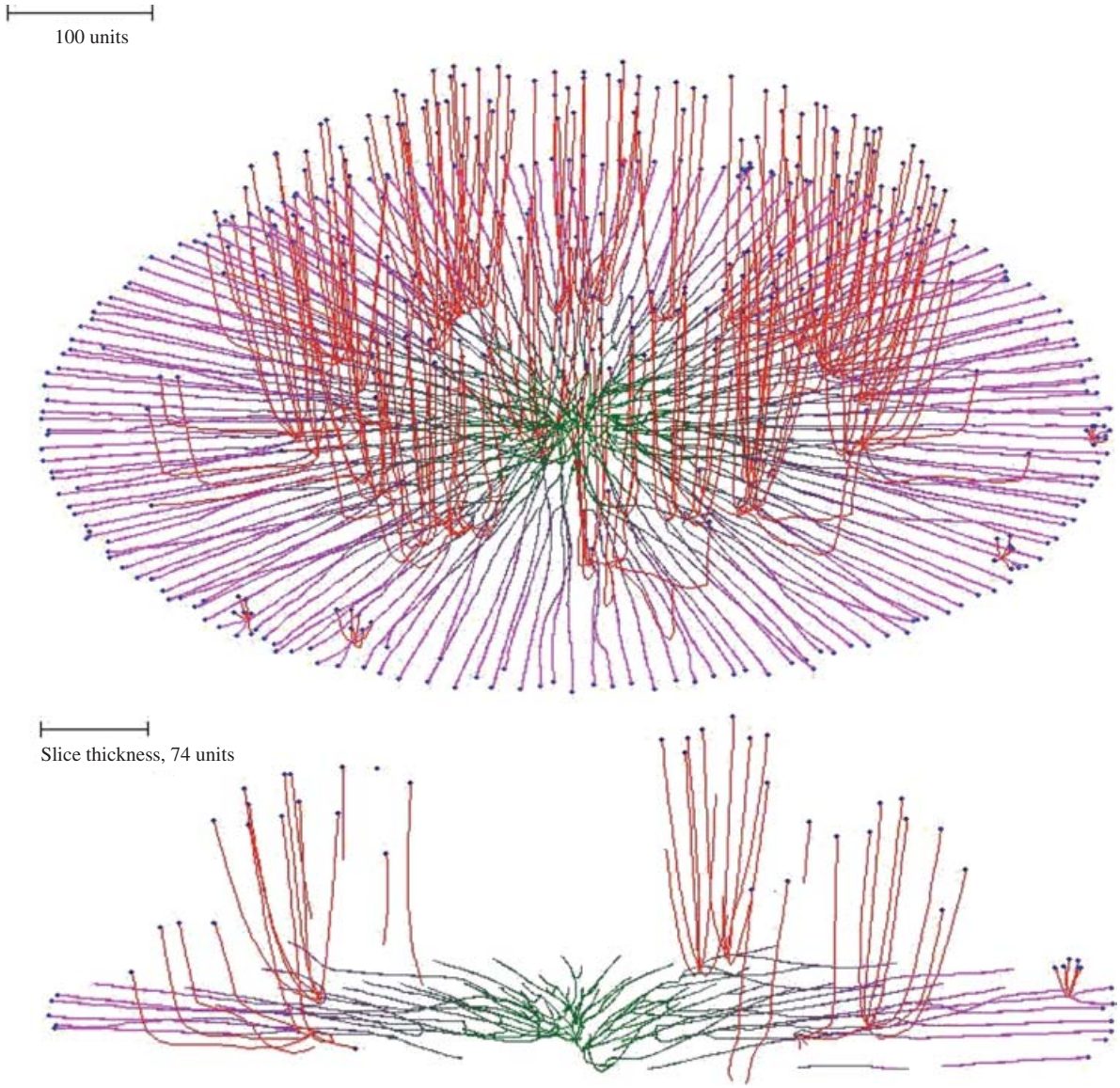

Fig. 9. Oblique view and slice of the colony, where secondary branching was activated at the 220 time unit. Differently from primary branches with horizontal tropism (impact constant 0.0007, zone height 4 units) the secondary branches had the negative gravitropism (impact constant 0.002). For both primary and secondary branches the growth was simulated assuming negative autotropic reaction (persistence factor $k = 0.1$) and density-dependent branching. The branching threshold was 0.06 at the apex and 0.12 at the old branch points forming secondary branches (max 8 new branches per branch point). Density field was generated by all mycelia ($l_c = 20$). If the density allowed branching, the branching probability was 40 % per iteration (per time unit). The final age of the colony is 294 time units. Secondary branches are colour-coded red, and hyphae of the primary mycelium are coloured green (oldest) to magenta (youngest), depending on the distance of the hyphal segment from the centre of the colony.

the centre of the mycelium, and because approaching hyphae have no reason to turn to grow in the same direction. Observations on cord formation between a bait and an inoculum by *Phanerochaete velutina* suggests that hyphae do indeed grow in both directions, so there seems to be some tolerance for uncertainty *in vivo*. However, the mathematical model requires a solution that does achieve concerted growth of linear structures and an approach that is successful in this is implementation of an orientation field.

The features required of an orientation field capable of forming linear structures are that it must be a vector field with direction running parallel to the direction of the linear structure we wish to create. Implementing a galvanotropism into the model solves this problem. From the literature it is evident that bacteria and fungi alike exhibit tropisms to electric fields and currents (Gruler & Gow 1990, Gow 1994, Gow & Morris 1995). Differentially-distributed ion pumps produce ion currents that leave the growing hyphal apex and re-enter the hypha at more basal regions. Hence, at least in some regions the lines of force of the corresponding electric field may be close to parallel to the hyphal axis. Such a field has the needed directionality that can be

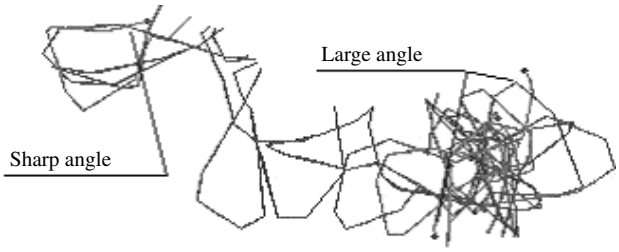

Fig. 10. The trajectory of a hyphal tip as it approaches other hyphae strongly depends on its angle of approach. An acute angle of approach may cause the approaching hyphal tip to curl in a spiral around the hypha it is approaching (left-hand illustration). An obtuse approach angle results in the approaching tip randomly orbiting its target (right-hand image).

used for orientation. Because the lines of force of the field from each hypha are oriented in the same direction the shared field of any linear structure formed in response to such a field can be much stronger than a single hypha is able to generate. Consequently, hyphal recruitment to a developing cord will be a self-accelerating process. Mycelial cords are one of a series of linearised hyphal structures that start with strands (poorly organised cords) and end with rhizomorphs (highly differentiated cords that in some fungi may be indistinguishable from fruit body stems) (Moore 1998: 249–254). Corded systems are capable of growing across dry inert substrates which would constrain the pathway for any circulating currents to a very local domain comprising the extracellular matrix and fluid filled spaces between the hyphae (Moore 1998: 261). These intercellular fluids could provide the electrical connections within and between the hyphae of an aggregate capable of supporting the galvanotropic signals. Indeed, since the nature of the matrix is under the control of the hyphae that produce it, the immediate extracellular environment of a living fungus offers scope for entertaining discussion of the dielectric characteristics of the matrix. We wish to stress that although an electric field seems a likely candidate for this particular tropism (and we refer to it as a galvanotropism), the mathematical model employs an abstract definition of the orientation field that is not dependent on any particular mechanism of generation and/or perception. Other mechanistic hypotheses are not excluded providing they can generate a directional field parallel to the hyphal long axis.

The specific features of this galvanotropism as implemented in the program result from the assumption that each hyphal segment, short enough to be considered as a straight line, forms an orientation field. This field is directed toward the end that is closer to the segment's hyphal tip and is parallel to the hyphal long axis. The absolute value of the field at any given point is inversely proportional to the shortest distance from that point to the segment generating the field. The total field of a mycelium perceived at any given point is a vector sum of the fields generated by all such mycelial

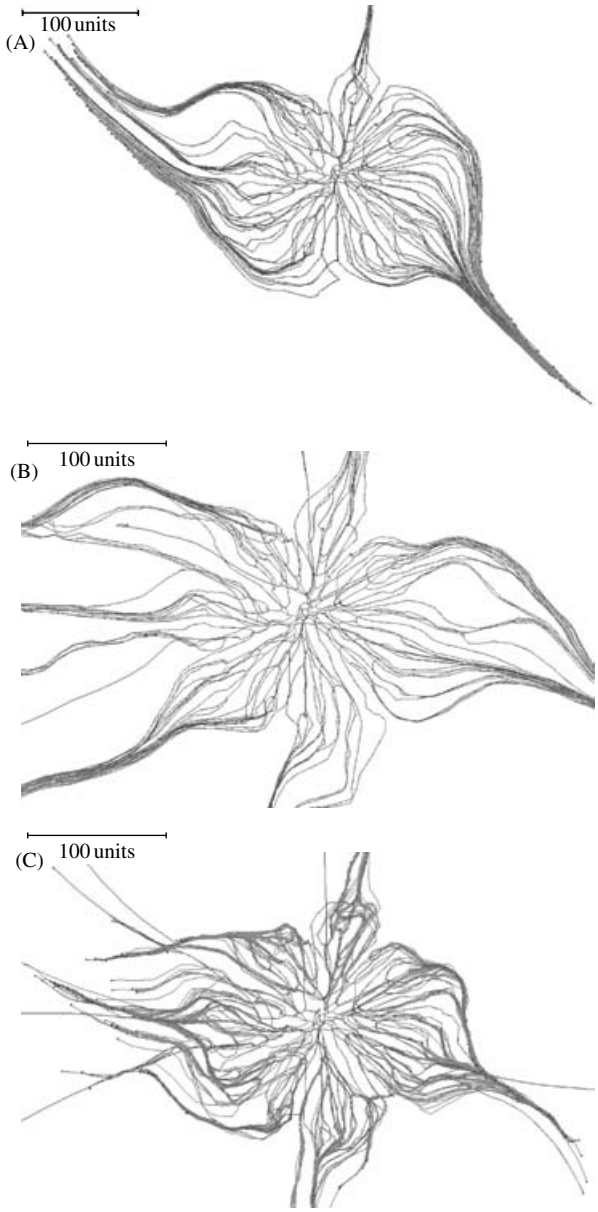

Fig. 11. Using the galvanotropic reaction to develop mycelial cords. Fig. 11A, the initial colony was grown for 98 time units with a parameter set that supposed negative autotropism, a tropism persistence factor of 0.1, density field-regulated branching (threshold of 0.06), probability of branching of 40 % per time unit, growth rate proportional to length (proportionality coefficient 0.1, maximum 5 length units per time unit), density field generated by all of the mycelium. A horizontal plane tropism was implemented to limit the hyphal tips to a horizontal layer with a thickness of 40 standard distance units. After the 98 time units the galvanotropism was activated (impact factor 0.1) together with the corresponding positive tropism (impact factor 0.15). Fig. 11B, development of cords using leading hyphae. Probability of the new branch becoming a leading hypha was set to 10 %. Leading branches (blue) lack galvanotropic sensitivity; other parameters as for Fig 11A. Fig. 11C, development of cords with leading branches and allowing secondary branching (so that cords can arise from within the mature regions of the colony). The density field threshold for secondary branching was 4 times higher than that set for standard or leading hyphae. Other parameters were identical to those used for the simulation in Fig. 11B.

segments. Implementing this feature in the Neighbour-Sensing model is sufficient to switch the morphology of the simulation from a diffuse spreading fan-like mycelium to a mycelium forming aggregated structures similar to strands and cords (Fig. 11).

Fig. 11A shows that the basic model does not require any additional assumptions to generate cords analogous to those formed by *Phanerochaete in vivo* (shown in Fig. 12), but there is a considerable amount of evidence to indicate that in real mycelia leading hyphae can organise cord formation around themselves, and cords can be formed from within the mature regions of a colony. Introducing the concepts of leading and secondary hyphae into the program enables simulation of these circumstances. If leading hyphae in the simulation are set to lack the galvanotropic response they do not join cords that are being formed, but instead become the initiating centres for cord formation (Fig. 11B).

Secondary branches are initiated at previous branch points if the local density is below the branching threshold set by the user. Mycelia formed by growing and branching of standard hyphae are usually dense enough to suppress secondary branching, so the model supports an additional constant that enables the user to define a difference in value between the critical hyphal density field controlling standard and secondary branching. Adding secondary branching to the cord-forming parameter set produces a colony that forms cords from both the peripheral and central regions (Fig. 11C).

In vivo, *Phanerochaete* progresses through three morphological phases: first, radially symmetric fine hyphae for perhaps 15–20 mm (Fig. 12A); second, establishment of cords from with this network and further growth as a fan of fine hyphae consolidating behind the margin as a cord (Fig. 12B & C), and, finally, a transition to growth almost exclusively as cords with very little spreading at the apex of the cord but a more obtuse branching angle. The early stages of corded growth are apparent in Fig. 12D, particularly from leading hyphae on the left half of the figure. Comparing Figs 11 and 12 suggests that the Neighbour-Sensing model can generate quite realistic strand-like and cord-like structures, but they dominate the mycelium in an unrealistic fashion. We believe that the key to the low level of visual similarity is most probably the number of hyphal tips involved in the simulation. There must be many thousands of hyphal tips in the live cultures, but a single processor computer cannot deal effectively with a visualization comprised of this number of tips. Parallel processing will be required to grow a colony to, say, 4000–5000 tips before imposing galvanotropic leaders with limited impact. This is a task for the future.

Implementing these cord formation parameters without constraining mycelia to stay in a single plane forms a bush-like structure, which is reminiscent of the shape of some lichens and the aerial rhizomorph networks found in tropical rain forests (Fig. 13A). Interestingly, when substrates were included in the visualization (to simulate leaf-catching by the rhizomorph network) the growing cord exhibited an unexpectedly high persistence factor, and in attempting to hit the substrate, it tended to miss the target and orbit it instead (Fig. 13B). After completing a single circle, such a structure behaved like an electric solenoid, generating a circular parallel field. This solenoid forced the growing tips to circle around infinitely, forming a dense ring at a specific distance from the substrate. This is an interesting demonstration of an inevitable but unforeseen consequence of assigning particular (in this case, electrical) properties to a biologically active tropic field, and is a clear illustration of the value of this sort of modelling. Evidently, galvanotropism alone does not provide an adequate simulation of the behaviour of rhizomorph networks, and further work would be required to make the behaviour of the simulations more lifelike.

Cyberspecies models

The evident similarities between Figs 11 and 12 encourage the belief that this model is now sufficiently advanced for parameters to be defined that simulate specific *in silico* cyberfungi. Fig. 11 is representative of what we would call a *cyberPhanerochaete*. Essentially, simulation of any *in vivo* system is feasible because the parameter options in the current mathematical model provide the means to achieve a great diversity of colony morphologies in biologically meaningful ways. It should be possible to collect other published growth characteristics (e.g. for *cyberRhizoctonia* by Boswell *et al*. 2002, 2003a, b) to incorporate into the program parameters that will provide realistic visualizations of several other fungi that are widely used for *in vivo* experimentation so that the user has immediate access to them.

Almost every modeller claims that the pattern produced by their model is realistic, despite the fact that the models incorporate vastly different assumptions and use completely different aspects of mycelial development in their simulations. They can't all be right, so it will be essential to develop statistical methods to compare *in vivo* and *in silico* hyphal patterns to validate objectively all claims for model realism. The potential utility of these cyberspecies is so great that such efforts would be worthwhile.

Cyberspecies would provide a means to model the morphogenetic effects of a variety of factors, from environmental and nutritional features to mutations, in experimentally realistic situations. Such tailored species models could be valuable additions to the experimental toolkit of all those interested in fungal growth and morphology. Very little time is required with a modest desktop computer for many iterative cycles of testing a wide range of hypotheses *in silico* on the predicted colony morphology of, say, a branching mutant, which

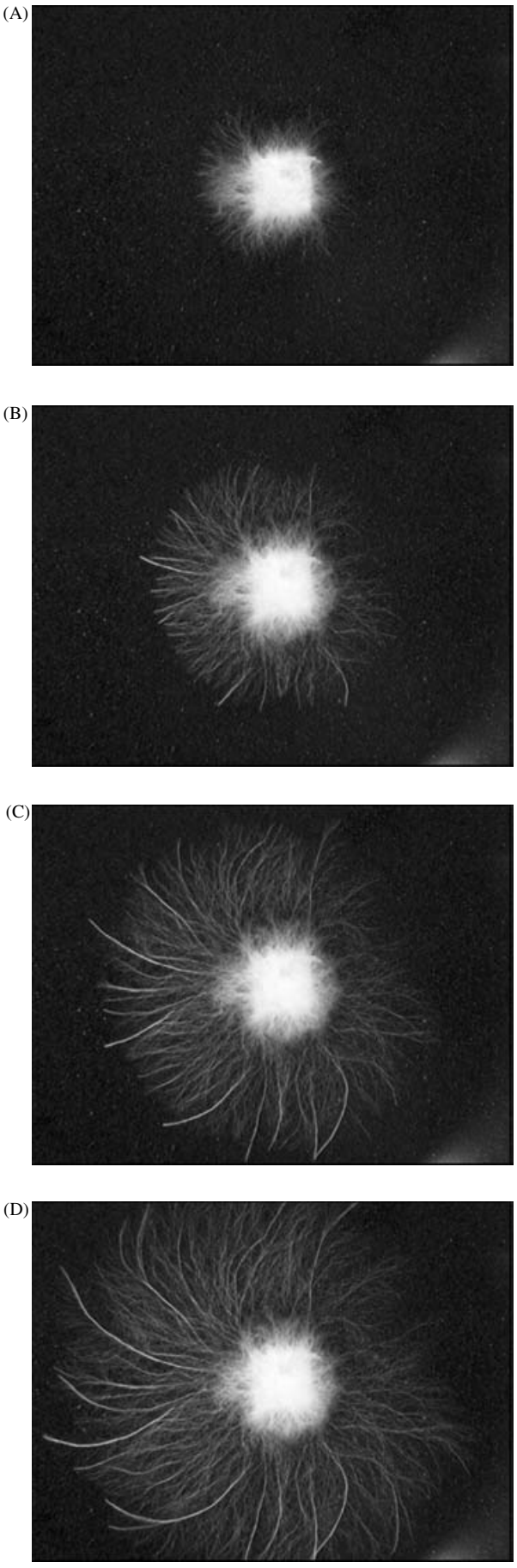

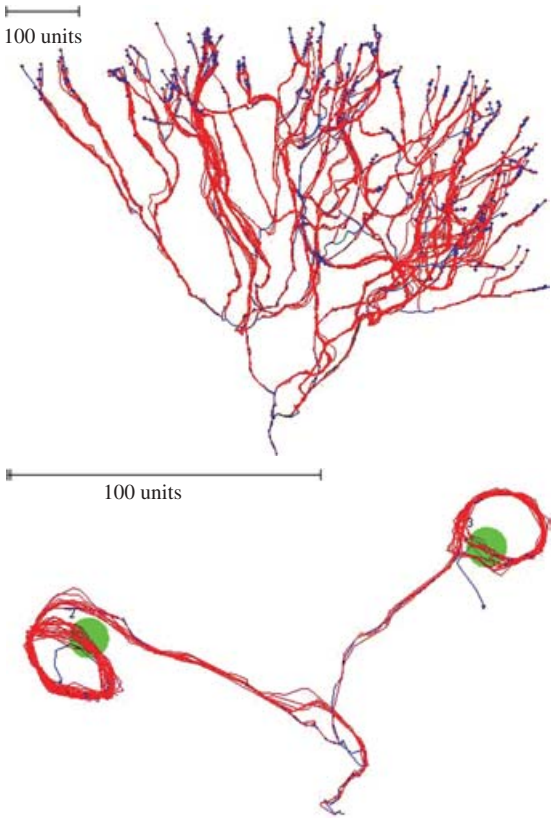

Fig. 13. Implementing the cord formation parameters without constraining the mycelium to stay in a single plane forms a bush-like structure (Fig. 13A, top), which is reminiscent of the shape of some lichen thalli and the rhizomorph networks of some tropical fungi. The mycelium consisted of standard and leading hyphae, the probability of the formation of leading hyphae was set to 50%. The standard hyphae were assigned both parallel and positive galvanotropisms (with impact 0.1), while leading hyphae were given a negative gravitropism instead (impact 0.002). In both cases the simulation assumed negative autotropism (persistence factor $k=0.1$) and density-dependent branching (threshold 0.06), the density field being generated by all of the mycelium ($l_c=20$). If the density allowed branching, the branching probability was set to 40% per iteration per time unit. Substrates (the green circles) were placed in the simulation shown in Fig. 13B (bottom). The substrates generated a positive tropic field (effectively equal to the autotropic field generated by a hyphal segment of 50 length units).

could then be experimentally validated with relatively simple *in vivo* measurements of Petri-dish cultures. The crucial *in vivo* measurement, of course, being chosen on the basis of the *in silico* survey.

Further developments of the Neighbour-Sensing model to enable it to simulate these fungi even more realistically would include hyphal senescence and hyphal anastomosis. The latest version of the model

Fig. 12. *Phanerochaete velutina* growing from a 1 cm^3 wooden block across black sand. The images were taken 144 h (12A), 192 h (12B), 240 h (12C) and 288 h (12D) after the start of the experiment.

provides the opportunity to remove hyphae from an established mycelium. The user decides that hyphal segments should be removed if the density field value at the tip exceeds a certain threshold value and/or if the number of tips supported by the section is less than the given threshold value. Removal proceeds in a basipetal direction from the hyphal tip that qualifies for removal to the closest branch point that does not qualify. Hyphal removal can be implemented after some delay (to avoid jeopardising initial growth of the mycelium) by the user setting minimum and maximum age of a hyphal section and/or minimum and maximum length of a hyphal section. The user can also decide whether the program should discard the data and remove the 'dead' branches from the visualization, or keep references to the dead branches. In the latter case a hyphal branch that is deemed to be dead (by the criteria set as above) does not contribute to the hyphal density field, but remains on display in the visualization in a unique colour.

A feature that remains to be implemented in the model is hyphal anastomosis. We are working on the mathematics of this and are confident that hyphal fusion can be catered for in the algorithms underlying the Neighbour-Sensing model. Inclusion of anastomosis will enable the model to generate biologically inspired networks and so provide a tool to analyse these networks to yield information about connectivity, minimum path length, etc. In addition it would be possible to address network robustness *in silico* by investigating the effect of removal of network links on connectivity. Looking further into the future, it should be possible to add physiological transaction 'costs' to growth and branching, catered for by substrate uptake and transport components. Since the Neighbour-Sensing model 'grows' a realistic mycelium and tracks all of the hyphal segments so generated, there is no mathematical impediment to assigning to those hyphal segments the algebraic characteristics defined to describe substrate uptake, utilization and translocation kinetics (Boswell *et al*. 2002, 2003a, b). The computation load would be extremely large; nevertheless, the ultimate model could be something akin to computer models of the atmosphere and be able not only to simulate the growth of a mycelium but also to plot its use of substrates, and accumulation, translocation and redistribution of resources.

ACKNOWLEDGEMENTS

We thank Liam J. McNulty for his help with some of the experiments reported here. In addition we acknowledge helpful discussion with Peter Darrah, and funding received from NERC (A/S/2002/00882) and EPSRC (GR/S63090/01).

REFERENCES

Boswell, G., Jacobs, H., Davidson, F., Gadd, G. M. & Ritz, K. (2002) Functional consequences of nutrient translocation in mycelial fungi. *Journal of Theoretical Biology* **217**: 459–477.

Boswell, G., Jacobs, H., Davidson, F., Gadd, G. M. & Ritz, K. (2003a) A positive numerical scheme for a mixed-type partial differential equation model for fungal growth. *Applied Mathematics and Computation* **138**: 321–340.

Boswell, G., Jacobs, H., Davidson, F., Gadd, G. M. & Ritz, K. (2003b) Growth and function of fungal mycelia in heterogeneous environments. *Bulletin of Mathematical Biology* **65**: 447–477.

Davidson, F. A. (1998) Modelling the qualitative response of fungal mycelia to heterogeneous environments. *Journal of Theoretical Biology* **195**: 281–292.

Davidson, F. A. & Olsson, S. (2000) Translocation induced outgrowth of fungi in nutrient-free environments. *Journal of Theoretical Biology* **205**: 73–84.

Davidson, F. A., Sleeman, B. D., Rayner, A. D. M., Crawford, J. W. & Ritz, K. (1996) Context-dependent macroscopic patterns in growing and interacting mycelial networks. *Proceedings of the Royal Society of London B* **263**: 873–880.

Edelstein, L. (1982) The propagation of fungal colonies: a model for tissue growth. *Journal of Theoretical Biology* **98**: 697–701.

Edelstein, L. & Segal, L. A. (1983) Growth and metabolism in mycelial fungi. *Journal of Theoretical Biology* **104**: 187–210.

Edelstein-Keshet, L. & Ermentrout, B. (1989) Models for branching networks in two dimensions. *SIAM Journal on Applied Mathematics* **49**: 1136–1157.

Ermentrout, G. B. & Edelstein-Keshet, L. (1993) Cellular automata approaches to biological modeling. *Journal of Theoretical Biology* **160**: 97–133.

Gow, N. A. R. (1994) Growth and guidance of the fungal hypha. *Microbiology* **140**: 3193–3205.

Gow, N. A. R. & Morris, B. M. (1995) The electric fungus. *Botanical Journal of Scotland* **47**: 263–277.

Gruler, H. & Gow, N. A. R. (1990) Directed growth of fungal hyphae in an electric field: a biophysical analysis. *Zeitschrift für Naturforschung* **45**: 306–313.

Hutchinson, S. A., Sharma, P., Clarke, K. R. & Macdonald, I. (1980) Control of hyphal orientation in colonies of *Mucor hiemalis*. *Transactions of the British Mycological Society* **75**: 177–191.

Lejeune, R. & Baron, G. V. (1997) Simulation of growth of a filamentous fungus in 3 dimensions. *Biotechnology and Bioengineering* **53**: 139–150.

Lejeune, R., Nielsen, J. & Baron, G. V. (1995) Morphology of *Trichoderma reesei* QM 9414 in submerged cultures. *Biotechnology and Bioengineering* **47**: 609–615.

Liddell, C. M. & Hansen, D. (1993) Visualizing complex biological interactions in the soil ecosystem. *Journal of Visualization and Computer Animation* **4**: 3–12.

Lindenmayer, A. (1968) Mathematical models for cellular interaction in development, Parts I and II. *Journal of Theoretical Biology* **18**: 280–315.

López, J. M. & Jensen, H. J. (2002) Generic model of morphological changes in growing colonies of fungi. *Physical Reviews, E* **65**: art. no.-021903.

Meškauskas, A., McNulty, L. J. & Moore, D. (2004) Concerted regulation of all hyphal tips generates fungal fruit body structures: experiments with computer visualizations produced by a new mathematical model of hyphal growth. *Mycological Research* **108**: 341–353.

Moore, D. (1984) Positional control of development in fungi. In *Positional Controls in Plant Development* (P. W. Barlow & D. J. Carr, eds): 107–135. Cambridge University Press, Cambridge, UK.

Moore, D. (1991) Perception and response to gravity in higher fungi – a critical appraisal. *New Phytologist* **117**: 3–23.

Moore, D. (1993) Control of pattern and form in mushroom morphogenesis. In *Mushroom Biology and Mushroom Products* (S. T. Chang, J. A. Buswell & S. W. Chiu, eds): 33–39. The Chinese University Press, Hong Kong.

Moore, D. (1994) Tissue formation. In *The Growing Fungus* (N. A. R. Gow & G. M. Gadd, eds): 423–465. Chapman & Hall, London.

Moore, D. (1998) *Fungal Morphogenesis*. New York: Cambridge University Press.

Moore, D., Hock, B., Greening, J. P., Kern, V. D., Novak Frazer, L. & Monzer, J. (1996) Gravimorphogenesis in agarics. *Mycological Research* **100**: 257–273.

Novak-Frazer, L. (1996) Control of growth and patterning in the fungal fruiting structure. A case for the involvement of hormones. In *Patterns in Fungal Development* (S. W. Chiu & D. Moore, eds): 156–181. Cambridge University Press, Cambridge, UK.

Prosser, J. I. (1995) Kinetics of filamentous growth and branching. In *The Growing Fungus* (N. A. R. Gow & G. M. Gadd, eds): 301–318. Chapman & Hall, London.

Prosser, J. I. & Trinci, A. P. J. (1979) A model for hyphal growth and branching. *Journal of General Microbiology* **111**: 153–164.

Prusinkiewicz, P. (1994) Visual models of morphogenesis. *Artificial Life* **1**: 61–74.

Prusinkiewicz, P. (2004) Modeling plant growth and development. *Current Opinion in Plant Biology* **7**: 79–83.

Prusinkiewicz, P. & Lindenmayer, A. (1990) *The Algorithmic Beauty of Plants*. Springer-Verlag, New York.

Regalado, C. M., Crawford, J. W., Ritz, K. & Sleeman, B. D. (1996) The origins of spatial heterogeneity in vegetative mycelia: a reaction-diffusion model. *Mycological Research* **100**: 1473–1480.

Reijnders, A. F. M. (1977) The histogenesis of bulb and trama tissue of the higher basidiomycetes and its phylogenetic implications. *Persoonia* **9**: 329–362.

Reijnders, A. F. M. (1993) On the origin of specialised trama types in the *Agaricales*. *Mycological Research* **97**: 257–268.

Soddell, F., Seviour, R. & Soddell, J. (1995) Using Lindenmayer systems to investigate how filamentous fungi may produce round colonies. *Complexity International* [ISSN 1320-0682]; on line at http://journal-ci.csse.monash.edu.au/ci/vol02/f_soddel/.

Tunbridge, A. & Jones, H. (1995) An L-Systems approach to the modeling of fungal growth. *Journal of Visualization and Computer Animation* **6**: 91–107.

Watling, R. & Moore, D. (1994) Moulding moulds into mushrooms: shape and form in the higher fungi. In *Shape and Form in Plants and Fungi* (D. S. Ingram & A. Hudson, eds): 270–290. Academic Press, London.

Yang, H., King, R., Reichl, U. & Gilles, E. D. (1992a) Mathematical model for apical growth, septation, and branching of mycelial microorganisms. *Biotechnology and Bioengineering* **39**: 49–58.

Yang, H., Reichl, U. & Gilles, E. D. (1992b) Measurement and simulation of the morphological development of filamentous microorganisms. *Biotechnology and Bioengineering* **39**: 44–48.

Corresponding Editor: N. P. Money